Frontiers in Heat and Mass Transfer (FHMT), 9, 30 (2017)
DOI: 10.5098/hmt.9.30

Global Digital Central
ISSN: 2151-8629

Frontiers in Heat and Mass Transfer

Available at www.ThermalFluidsCentral.org

MHD NANOFLUID FLOW WITH VISCOUS DISSIPATION AND JOULE HEATING THROUGH A PERMEABLE CHANNEL

Habib-Olah Sayehvand[a], Shirley Abelman [b,*], Amir Basiri Parsa[a]

[a] *Mechanical Engineering Department, Bu-Ali Sina University, Hamedan, 65174, Iran.*
[b] *School of Computer Science and Applied Mathematics and DST-NRF Centre of Excellence in Mathematical and Statistical Sciences, University of the Witwatersrand, Johannesburg, Private Bag 3, Wits 2050, South Africa.*

ABSTRACT

Magnetohydrodynamic (MHD) nanofluid flow considered to be steady, incompressible and electrically conducting, flows through permeable plates in the presence of convective heating, models as a system of nonlinear partial differential equations which are solved analytically by the Differential Transform Method (DTM). Copper, aluminum oxide and titanium dioxide nanoparticles are considered with Carboxyl Methyl Cellulose (CMC)–water as the base fluid. Variation of the effects of pertinent parameters on fluid velocity and temperature is analyzed parametrically. Verification between analytical (DTM) and numerical (fourth-order Runge-Kutta scheme) results and previous published research is shown to be quite agreeable. The temperature of Cu-water is found to be low in comparison with Al_2O_3-water and TiO_2-water which is reasonable for high thermal conductivity of copper. Furthermore increasing the volume fraction of nanoparticles causes enhancement of thermal conductivity and decrease in temperature.

Keywords: *Analytical solution; magnetohydrodynamic; Nanofluid; Permeable plates; viscous dissipation.*

1. INTRODUCTION

Increasing the coefficient of heat transfer is important for all industrial applications. Ultra-high-performance can be obtained by suspending ultrafine solid particles in a convectional fluid. The thermal conductivity of solid metals is larger than fluids; therefore suspending these particles can increase thermal conductivity and heat transfer performance. Several studies have been conducted this field as presented by Choi and Eastman (1995) experimentally and numerically (e.g., Rasidi et al., 2015; Rashidi *et al.*, 2014). Li and Xuan (2002) reported a 60% increment in convective heat transfer of fluid inside a channel filled with suspended nano-size copper particles with 3% volume fraction, compared to pure fluid. Based on our knowledge, Choi (1995) was the first person who experimentally verified that addition of nanoparticles to conventional base fluids enhanced thermal conductivity. Then other experimental results (e.g., Choi et al., 2001; Das *et al.*, 2007) have also illustrated that thermal conductivity of these nanofluids can be increased considerably via the introduction of nanoparticles. Because of its fundamental importance in engineering systems, entropy generation encountered in flows inside a channel has been studied by many researchers (e.g., Chamkha, 1995; Teamah, 2008).

Based on different scientific and practical applications in different industrial areas, the study of two-dimensional boundary layer flow, heat and mass transfer over a porous surface is quite important. The effect of viscous dissipation is to change the temperature distribution by acting like an energy source. The merit of the viscous dissipation effect depends on whether the plate is being cooled or heated. Apart from viscous dissipation in MHD flows, Joule dissipation also plays a role like a volumetric heat source. Heat transfer analysis of flow over a porous surface has received much practical interest with abundant applications. Specifically, heat-treated materials traveling between a feed roll and wind-up roll or materials manufactured by extrusion, glass-fiber and paper production, cooling of metallic sheets or electronic chips, crystal growing just to name a few. In these cases, the final desired characteristics depend on the rate of cooling in the process. To appreciate all these aspects, the present work deals with the effect of viscous and Joule dissipation on MHD flow of three different kinds of nanofluids, heat and mass transfer through a channel. Abdulla (2011) investigated theoretically and experimentally composite materials under the influence of thermal insulation. Reddy et al. (2009), studied thermal diffusion and Joule heating effects with simultaneous thermal and mass diffusion in MHD mixed convection flow. Combined forced and free flow analysis in a vertical channel with viscous dissipation was studied by Barletta (1999). Pandey and Kumar (2016) investigated the effects of viscous dissipation and suction/injection on MHD flow of a nanofluid past a wedge with convective surface in the appearance of slip flow and porous medium. Babu and Sandeep (2016) carried out a theoretical analysis to investigate free convective heat and mass transfer in three-dimensional MHD nanofluid flow over a stretching sheet in the presence of thermophoresis and Brownian motion effects. Joule heating in MHD flow through channels was investigated by Mao et al. (2008). Pandey and Kumar (2017) examined the collective influence of thermal radiation and convection flow of Cu-water nanofluid due to a stretching cylinder in a porous medium along with viscous dissipation and slip boundary conditions. Animasaun and Sandeep (2016) investigated nanofluid flow in the presence of nonlinear thermal radiation, Lorentz force and space dependent internal heat source within thin boundary layer. Ravikumar et al. (2012) studied Couette MHD flow over a porous

* *Corresponding author. Email: Shirley.Abelman@wits.ac.za*

Global Digital Central
ISSN: 2151-8629

plate with heat transfer. A theoretical investigation of MHD fluid flow, heat and mass transfer with Brownian and thermophoresis effects, with variable magnetic fields was carried out by Raju et al. (2016). Mixed convection inside a lid-driven cavity with heating was considered by Sumon et al. (2010). Krishna et al. (2016) presented a numerical solution for heat and mass transfer in unsteady Powell-Eyring fluid flow over a plate with suction/injection effects. Also, the consequences of heat generation/absorption and suction/injection on MHD flow of Ag-water nanofluid past a stretching flat plat in a porous medium with Ohmic-viscous dissipation were identified by Upreti et al. (2017).

Most scientific phenomena which have been modeled mathematically by governing equations such as Navier–Stokes problems are nonlinear. Explicit solution of these nonlinear equations is fundamentally important. Limited numbers of these problems have precise analytical solutions; usually these nonlinear equations should be solved using other methods. In recent decades, many efforts have been made to develop better methods to determine an analytical solution of these equations. One of the basic techniques is the differential transform method (DTM), which is based on Taylor series expansions. In 1986, Zhou (1986) employed the basic ideas of DTM for solving both linear and nonlinear problems in the field of electrical circuit problems. It gives exact values of the n th derivative of an analytical function at a point in terms of known and unknown boundary conditions in a fast manner. Chen and Ho (1999) developed this method for partial differential equations and Ayaz (2004) applied it to a system of ordinary differential equations. Jang et al. (2001) presented the two-dimensional DTM for partial differential equations. Subsequently, this method was successfully applied to various application problems (e.g., Erfani et al., 2010; Basiriparsa et al., 2013).

The purpose of the present paper is to solve the problem of MHD nanofluid flow through a channel with the permeable plates with hydrodynamic slip and convective boundary conditions by taking viscous dissipation and Joule heating into account. The governing equations are solved by analytical and numerical methods. Since this problem using a pure fluid instead of a nanofluid was solved numerically by Ibánez (2015), his results are used as a comparison reference for our study. In our analytical solution, a final solution as a closed form solution is presented and the obtained results are verified numerically.

2. GENERAL GUIDELINES

An incompressible viscous nanofluid which is electrically conducting flows in a channel steadily and fully developed. The horizontal channel consists of two parallel permeable plates at a distance $2a$ apart. There is a constant longitudinal pressure gradient dp/dx' and a uniform transverse magnetic field B0 perpendicular to the plates. The upper plate is located at $y' = a$ and the lower plate is at $y' = -a$ with y' denoting the transversal coordinate. The parallel plates are assumed to be infinite; therefore the velocity and temperature profiles are fully developed. The fluid is injected uniformly into the channel from the lower plate and fluid suction occurs at the upper plate. There is convective heat exchange by hot fluid with temperature T_h through the lower plate, while the upper plate is in contact with the ambient. It is assumed that the velocity profile satisfies the slip condition at the plates to solve the momentum balance equation, and the heat transfer equation is solved using third kind boundary conditions. The fluid is CMC–water-based with concentration (0.1–0.4%) containing three types of nanoparticles Cu, , Al_2O_3 and TiO_2. Nanofluid flow is assumed to be laminar and the base fluid and the nanoparticles are in thermal equilibrium. The thermophysical properties of the nanofluid are displayed in Table 1 (e.g., Das et al., 2015). A schematic view of the MHD channel with the permeable plates is shown in Fig. 1.

Under the above assumptions, the governing equations of momentum and energy can be written (Das and Jana, 2014; Das et al., 2015; Vyas and Soni, 2016)

$$v_0 \frac{du'}{dy'} = -\frac{1}{\rho_{nf}}\frac{dP}{dx'} + \frac{\mu_{nf}}{\rho_{nf}}\frac{d^2u'}{dy'^2} - \frac{\sigma_{nf} B_0^{\,2}}{\rho_{nf}}u', \tag{1}$$

$$v_0 (\rho c_p)_{nf} \frac{dT}{dy'} = k_{nf}\frac{d^2T}{dy'^2} + \mu_{nf}\left(\frac{du'}{dy'}\right)^2 + \sigma_{nf} B_0^{\,2} u'^2, \tag{2}$$

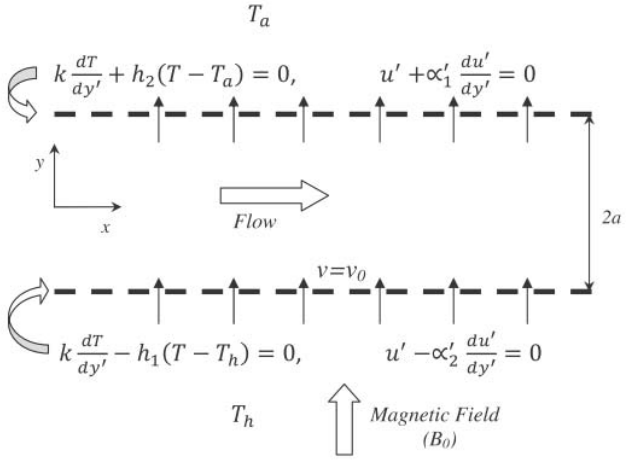

Fig. 1 Schematic of the problem and coordinate system.

Table 1 Thermophysical properties of the base fluid and the nanoparticles (e.g., Das et al., 2015).

Physical properties	*CMC-water*	*Cu*	Al_2O_3	TiO_2
$C_p(J/kg\ K)$	4179	385	765	686.2
$\rho(kg/m^3)$	997.1	8933	3970	4250
$k(W/m\ K)$	0.613	400	40	8.954
$\sigma(S/m)$	5.5×10^{-6}	59.6×10^{6}	35×10^{6}	2.6×10^{6}

Since the plates have different surface roughness, the slip lengths, although taken to be constant, do not have the same value on the upper and lower plates. Therefore, the boundary conditions are (Eegunjobi and Makinde, 2012; Chinyoka and Makinde, 2013)

$$\begin{aligned} &u' - \alpha_1'\frac{\partial u'}{\partial y'} = 0,\ k_{nf}\frac{\partial T}{\partial y'} - h_1(T - T_h) = 0, \quad \text{at } y' = -a, \\ &u' + \alpha_2'\frac{\partial u'}{\partial y'} = 0,\ k_{nf}\frac{\partial T}{\partial y'} + h_2(T - T_a) = 0, \quad \text{at } y' = a, \end{aligned} \tag{3}$$

where u' is the fluid velocity along the x – direction, T is the temperature of the nanofluid, v_0 is the uniform suction/injection velocity at the channel plates and a is the half distance between the plates while α_1' and α_2' are the slip lengths of the upper and lower plates, respectively, which in general, are assumed to be different. Also T_h is the hot fluid temperature, T_a is the ambient temperature, while h_1 and h_2 are the convective heat transfer coefficients for each plate. The third term on the right-had side of Eq. (2) is the Joule dissipation described in terms of the Ohm's law. In addition, μ_{nf} the dynamic viscosity of the nanofluid, ρ_{nf} the density of the nanofluid, σ_{nf} the electrical conductivity of the nanofluid, k_{nf} the thermal conductivity of the nanofluid and $(\rho c_p)_{nf}$ the heat capacitance of the nanofluid based on spherical nanoparticles are respectively given by Das et al., (2015), as follow

$$\mu_{nf} = \frac{\mu_f}{(1-\phi)^{2.5}}, \quad \rho_{nf} = (1-\phi)\rho_f + \phi\rho_s,$$
$$(\rho c_p)_{nf} = (1-\phi)(\rho c_p)_f + \phi(\rho c_p)_s,$$
$$\sigma_{nf} = \sigma_f\left[1+\frac{3(\sigma-1)\phi}{(\sigma+2)-(\sigma-1)\phi}\right], \ \sigma = \frac{\sigma_s}{\sigma_f}, \tag{4}$$
$$k_{nf} = k_f\left[\frac{k_s+2k_f-2\phi(k_f-k_s)}{k_s+2k_f+2\phi(k_f-k_s)}\right].$$

where ϕ is the solid volume fraction of nanofluid, ρ_f the density of the base fluid, ρ_s the density of the nanofluid, σ_f the electrical conductivity of the base fluid, σ_s the electrical conductivity of the nanofluid, μ_f the viscosity of the base fluid, $(\rho c_p)_f$ the heat capacitance of the base fluid and $(\rho c_p)_s$ the heat capacitance of the nanoparticle, where k_f is the thermal conductivity of the base fluid and k_s the thermal conductivity of the nanoparticle. In the above equations, the subscripts nf, f and s denote the thermophysical properties of the nanofluid, base fluid and nano-solid particles, respectively. To obtain the non-dimensional form of the above system of ordinary differential equations, the following dimensionless variables are introduced (Das and Jana, 2014; Das et al., 2015):

$$y = \frac{y'}{a}, \quad u = \frac{au'}{\nu_f}, \quad \theta = \frac{T-T_a}{T_h-T_a}, \quad \alpha_1 = \frac{\alpha_1'}{a}, \quad \alpha_2 = \frac{\alpha_2'}{a}. \tag{5}$$

Replacing these dimensionless variables into Eqs. (1) and (2) results in the nonlinear ordinary differential equations,

$$\frac{\nu_0\nu_f\rho_f}{a^2}\phi_1\frac{du}{dy} = -\frac{dp}{dx} + \frac{\mu_f}{(1-\phi)^{2.5}}\frac{\nu_f}{a^3}\frac{d^2u}{dy^2} - \frac{\sigma_f B_0^2\nu_f}{a}\phi_2 u, \tag{6}$$

$$\nu_0(\rho c_p)_f\frac{(T_h-T_a)}{a}\phi_3\frac{d\theta}{dy} =$$
$$k_{nf}\frac{(T_h-T_a)}{a^2}\frac{d^2\theta}{dy^2} + \frac{\mu_f}{(1-\phi)^{2.5}}\frac{\nu_f^2}{a^4}\left(\frac{du}{dy}\right)^2 + \frac{\sigma_f B_0^2\nu_f^2}{a^2}\phi_2 u^2. \tag{7}$$

After simplification Eqs. (6) and (7) become

$$S\phi_1\frac{du}{dy} - P - \frac{1}{(1-\phi)^{2.5}}\frac{d^2u}{dy^2} + M^2\phi_2 u = 0, \tag{8}$$

$$S.\Pr.\phi_3\frac{d\theta}{dy} - \frac{k_{nf}}{k_f}\frac{d^2\theta}{dy^2} - \Pr.Ec\left[\frac{1}{(1-\phi)^{2.5}}\left(\frac{du}{dy}\right)^2 + M^2\phi_2 u^2\right] = 0. \tag{9}$$

The boundary conditions become

$$u - \alpha_1\frac{du}{dy} = 0, \quad \frac{k_{nf}}{k_f}\frac{d\theta}{dy} - Bi_1(\theta-1) = 0 \quad at \ y = -1,$$
$$u + \alpha_2\frac{du}{dy} = 0, \quad \frac{k_{nf}}{k_f}\frac{d\theta}{dy} + Bi_2\theta = 0 \quad at \ y = 1, \tag{10}$$

where $Bi_1 = ah_1/k_f$, $Bi_2 = ah_2/k_f$ are the Biot numbers (or surface convection parameters) and α_1, α_2 are dimensionless slip lengths of the upper and lower plates, respectively. It is clear that for a permeable channel with different permeability, the slip velocity condition is more accurate than the no-slip condition. When $Bi_1, Bi_2 \to \infty$, the convective boundary condition reduces to a uniform surface temperature boundary condition. Further, $Bi_1, Bi_2 = 0$ correspond to insulated plates. When $Bi_1 = Bi_2$, the channel is cooled symmetrically and heat is dissipated equally from the left and right plates. Also

$$\phi_1 = \frac{\rho_{nf}}{\rho_f} = \left[(1-\phi)+\phi\left(\frac{\rho_s}{\rho_f}\right)\right],$$
$$\phi_2 = \frac{\sigma_{nf}}{\sigma_f} = \left[1+\frac{3(\phi-1)\phi}{(\phi+2)-(\phi-1)\phi}\right], \tag{11}$$
$$\phi_3 = \frac{(\rho c_p)_{nf}}{(\rho c_p)_f} = \left[(1-\phi)+\phi\frac{(\rho c_p)_s}{(\rho c_p)_f}\right],$$

And

$$S = \frac{v_0 a}{\nu_f} \ (\text{Suction parameter}),$$
$$P = \frac{a^3}{\nu_f^2\rho_f}\left(-\frac{dp}{dx}\right) \ (\text{Pressure gradiant parameter}),$$
$$M^2 = \frac{\sigma_f B_0^2 a^2}{\nu_f\rho_f} \ (\text{Magnetic parameter}), \tag{12}$$
$$Ec = \frac{\nu_f^2}{a^2 c_{p_f}(T_h-T_a)} \ (\text{Eckret number}),$$
$$\Pr = \frac{\rho_f c_{p_f}\nu_f}{k_f} \ (\text{Prandtl number}).$$

In this section the coupled system of nonlinear ordinary differential equations (9) is derived to model MHD nanofluid flow through a permeable wall channel in the presence of hydrodynamic slip and convective boundary condition. In the next section the DTM and numerical method (fourth-order Runge-Kutta scheme) are applied to solve this coupled system.

The shear stress, the rate of heat transfer and the rate of mass flux on the lower and upper plates can be written as

$$\tau_{w_{Lower}} = -\mu_{nf}\left.\frac{\partial u}{\partial y}\right|_{y=-a}, \quad \tau_{w_{Upper}} = -\mu_{nf}\left.\frac{\partial u}{\partial y}\right|_{y=a},$$
$$q_{w_{Lower}} = -k_{nf}\left.\frac{\partial T}{\partial y}\right|_{y=-a}, \quad q_{w_{Upper}} = -k_{nf}\left.\frac{\partial T}{\partial y}\right|_{y=a}, \tag{13}$$

The important parameters such as the skin coefficient friction (C_f) and Nusselt number (Nu) are derived from substituting the dimensionless variables in Eqs. (11), for the lower and upper plates:

$$C_{f_{Lower}} = \left|\frac{\mu_{nf}}{\mu_f}f''(-1)\right|, \quad C_{f_{Upper}} = \left|\frac{\mu_{nf}}{\mu_f}f''(1)\right|,$$
$$Nu_{Lower} = \left|\frac{k_{nf}}{k_f}\theta(-1)\right|, \quad Nu_{Upper} = \left|\frac{k_{nf}}{k_f}\theta(1)\right|, \tag{14}$$

3. ANALYTICAL APPROXIMATION BY DTM

Taking the differential transform of Eqs. (8) and (9), one obtains (for more details, see Rashidi et al. (2014))

$$S\phi_1(k+1)U(k+1) - P\delta(k) -$$
$$\frac{1}{(1-\phi)^{2.5}}(k+2)(k+1)U(k+2) + M^2\phi_2 U(k) = 0, \tag{15}$$

$$S.\Pr.\phi_3.(k+1)\Theta(k+1) - \frac{k_{nf}}{k_f}(k+2)(k+1)\Theta(k+2) -$$
$$\Pr.Ec.\left(\frac{1}{(1-\phi)^{2.5}}\sum_{r_1=0}^{k}[U(r_1+1)(r_1+1)(k+1-r_1)U(k+1-r_1)] + M^2\phi_2\sum_{r_2=0}^{k}[U(r_2)U(k+-r_2)]\right) = 0 \tag{16}$$

Global Digital Central
ISSN: 2151-8629

When $\delta(k)$ is the Kronecker delta defined as $\delta(k)=\begin{cases}1, & k=0,\\ 0, & k\neq 0.\end{cases}$. Also $U[k]$ and $\Theta[k]$ are differential transforms of $u(y)$ and $\theta(y)$ given by

$$u(y)=\sum_{k=0}^{\infty}U(k)\,y^{k}, \tag{17}$$

$$\theta(y)=\sum_{k=0}^{\infty}\Theta(k)\,y^{k}, \tag{18}$$

$$U(0)=C_1,\ U(1)=C_2,\quad \Theta(0)=C_3,\ \ \Theta(1)=C_4. \tag{19}$$

Where Eqs. (19) are the transformed boundary conditions and C_1, C_2, C_3 and C_4 are constants. By substituting Eqs. (19) into Eqs. (15) - (16), using recursion, and then substituting them into Eqs. (17) - (18), the values of $u(y)$ and $\theta(y)$ are

$$u(y)\approx C_1+C_3y+\frac{1}{2}(1-\phi)^{2.5}\left(C_1\phi_2M^2-P+C_2\phi_1S\right)y^2+\frac{1}{6}(1-\phi)^{2.5}\left(C_2\phi_2M^2+(1-\phi)^{2.5}\phi_1S\,(C_1\phi_2M^2-P+C_2\phi_1S)\right)y^3+..., \tag{20}$$

$$\theta(y)\approx C_3+C_4y+\frac{k_f}{2k_{nf}}\left(-Ec\left(\frac{C_2^{\,2}}{(1-\phi)^{2.5}}+C_1^{\,2}\phi_2M^2\right)\mathrm{Pr}+C_4.\phi_3\,\mathrm{Pr}.S\right)y^2+\frac{k_f}{6k_{nf}}\left(\begin{array}{l}\dfrac{k_f}{k_{nf}}\phi_3\,\mathrm{Pr}.S\left(-Ec\left(\dfrac{C_2^{\,2}}{(1-\phi)^{2.5}}+C_1^{\,2}\phi_2M^2\right)\mathrm{Pr}+C_4\phi_3\,\mathrm{Pr}.S\right)-\\ Ec.\mathrm{Pr}\left(2C_1C_2\phi_2M^2+2C_2(C_1\phi_2M^2-P+C_2\phi_1S)\right)\end{array}\right)y^3+... \tag{21}$$

The constants C_1, C_2, C_3 and C_4 can be determined by applying the remaining boundary conditions to Eqs. (20) - (21). The number of required terms is determined by the convergence of the numerical values to a desired accuracy. The approximants are obtained by employing the computational software MATHEMATICA. The effect of different orders of the DTM solution on the convergence radius of $u(y)$ and $\theta(y)$ is displayed in Figs. 2, 3.

4. COMPARISONS AND VERIFICATION

For a pure fluid (instead of a nanofluid) the present problem reduces to that of Ibánez (2015). In Figs. 2 and 3, the obtained velocity and temperature profiles are compared with those reported in Ibánez (2015). Also, these obtained results, for different orders of DTM, are compared with numerical results (obtained by fourth-order Runge-Kutta quadrature with a shooting method). Thermophysical properties of the base fluid and the nanoparticles are listed in Table 1. Very good agreement is found in the quantitative comparisons of the present analytical results (order 30 of DTM) and numerical solution in comparison with the previously published study (e.g., Ibánez, 2015) as shown in Figs. 2 and 3.

5. RESULTS AND DISCUSSION

Two different methods, DTM and numerical method are applied to the governing partial differential equations to derive semi-numerical solutions under appropriate boundary conditions. As can be seen in Figs. 2 and 3, good agreement between analytical and numerical results is obtained.

To present physical results from this study, the effect of different values of various parameters is discussed on fluid velocity and temperature profiles namely magnetic parameter M^2, pressure gradient parameter P, suction parameter S, Eckert number Ec, Biot numbers Bi_1 and Bi_2, dimensionless slip lengths α_1, α_2 and nanoparticle materials.

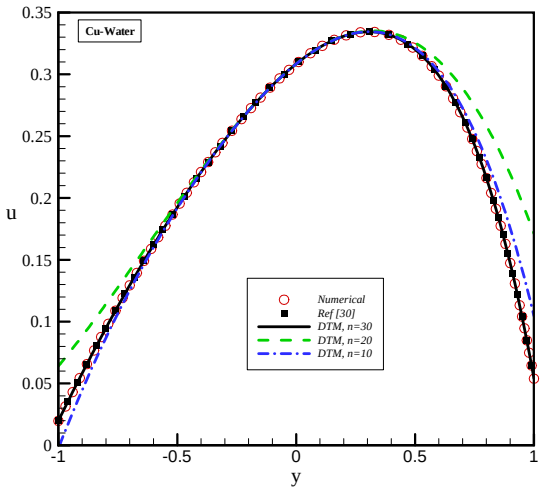

Fig. 2 Comparison between the DTM and numerical solution with previously published data (e.g., Ibánez, 2015) for velocities profile when $\phi=0,\ S=2,\ M^2=1,\ Ec=0.1,\ P=1,\ \mathrm{Pr}=6.2,\ \alpha_1=\alpha_2=0.01,\ Bi_1=Bi_2=100.$

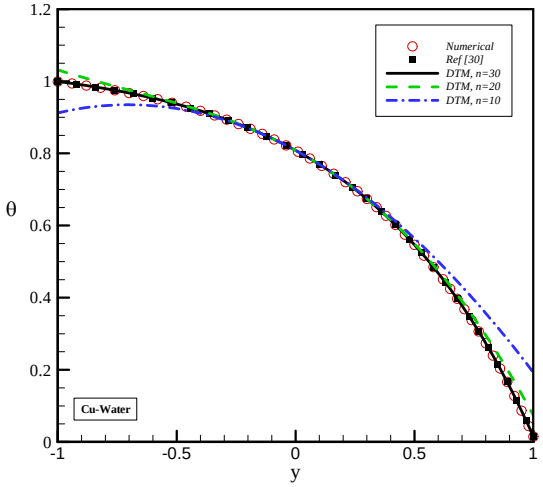

Fig. 3 Comparison between the DTM and numerical solution with previously published data (e.g., Ibánez, 2015) for temperature profile when $\phi=0,\ S=2,\ M^2=1,\ Ec=0.1,\ P=1,\ \mathrm{Pr}=6.2,\ \alpha_1=\alpha_2=0.01,\ Bi_1=Bi_2=100.$

The following results are obtained by DTM. The value of the Prandtl number for the base fluid is kept as $\mathrm{Pr}=6.2$ (room temperature) and the effect of solid volume fraction is investigated in the range $0\le\phi\le 0.15$. The case $M^2=0$ corresponds to the absence of magnetic field and $\phi=0$ for a regular fluid. $Ec=0$ presents no Joule and viscous heating. The main values of the governing parameters and their variation range are selected according to Table 2 and effects of each of them on the velocity, temperature and Nusselt number will be checked, separately.

Global Digital Central
ISSN: 2151-8629

Table 2 The main values of the governing parameters and their variation ranges.

Parameter	*Basic quantity*	*Range of changes*
magnetic parameter (M)	$M^2=1$	$1<M^2<2$
pressure gradient parameters (P)	$P=1$	$0.5<P<1$
suction parameter (S)	$S=0.5$	$0<S<0.7$
Eckert number (Ec)	$Ec=0.1$	$0.1<Ec<1$
dimensionless slip lengths (α_1,α_2)	$\alpha_1,\alpha_2=0.01$	$0.01<\alpha_1,\alpha_2<0.1$
Biot numbers (Bi_1,Bi_2)	$Bi_1,Bi_2=1$	$1<Bi_1,Bi_2<10$
nanoparticle volume fraction (ϕ)	$\phi=0.05$	$0<\phi<0.15$

5.1 Effect of parameters on velocity profile

Analyses of magnetic and pressure gradient parameters for Cu-water nanofluid are presented in Fig. 4. As can be seen in this figure, the main effect of the magnetic parameter, which gives an estimation of magnetic forces versus viscous forces, on the velocity profile is to make it flatter and decrease the velocity. By increasing in the pressure gradient, an increment in the velocity profile is observed. When the suction parameter increases, both the injection at lower plate and the suction at upper plate increase which causes the velocity profile to decrease and also causes this profile to skew towards the upper plate (see Fig. 5). Also, it is obvious that the velocity does not change with Eckert number Ec, because the Eckert number has no effect on the momentum equation.

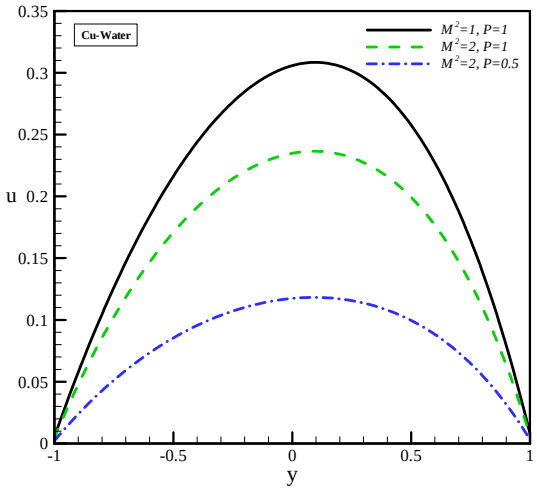

Fig. 4 Effect of M^2,P on the velocity profile when $\phi=0.05,\ S=0.5,\ Ec=0.1,\ \alpha_1=\alpha_2=0.01,\ Bi_1=Bi_2=1.$

Fig. 6 presents the effect of increasing both slip lengths on the velocity profile. According to the boundary conditions, raising the velocity on each side of the channel due to its slip lengths is predictable. Also since the Biot number has no effect on the momentum equation, it is clear that the velocity does not change with Biot numbers (Fig. 7). Fig. 8 shows the effect of nanoparticle volume fraction on velocity, for Cu-water. It can be seen that the dimensionless boundary layer velocity decreases by increasing the volume fraction due to loss of fluid flow inertia. Variations of fluid velocity for three types of water-based nanofluids Cu-water, Al_2O_3-water and TiO_2-water are illustrated in Fig. 9. Since the density of particles is not very different, the fluid velocity is almost the same.

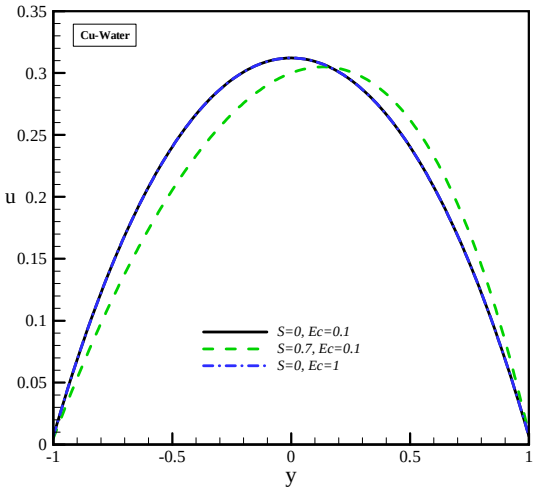

Fig. 5 Effect of S,Ec on the velocity profile when $\phi=0.05,\ M^2=1,\ P=1,\ \alpha_1=\alpha_2=0.01,\ Bi_1=Bi_2=1.$

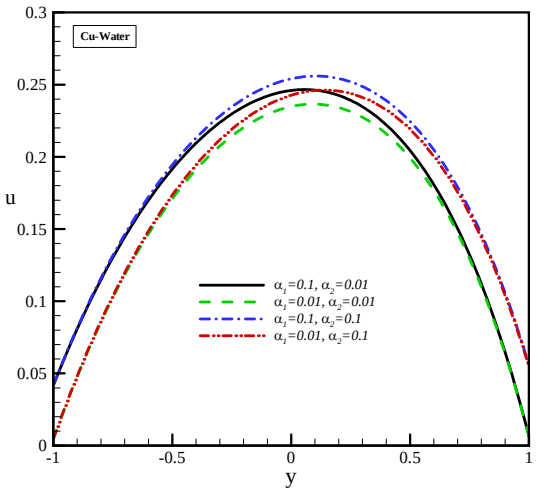

Fig. 6 Effect of α_1,α_2 on the velocity profile when $\phi=0.05,\ M^2=2,\ P=1,\ S=0.5,\ Ec=0.1,\ Bi_1=Bi_2=1.$

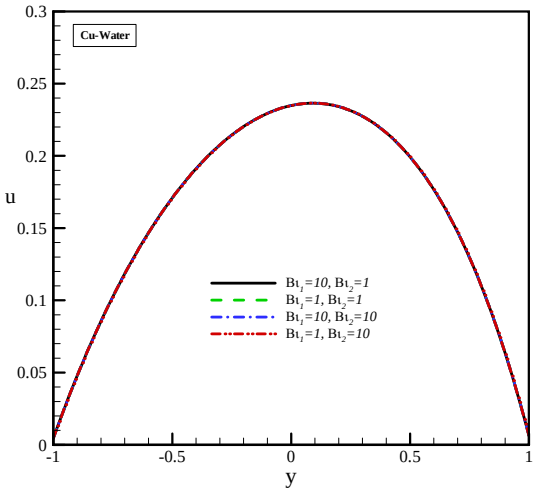

Fig. 7 Effect of Bi_1,Bi_2 on the velocity profile when $\phi=0.05,\ M^2=2,\ P=1,\ S=0.5,\ Ec=0.1,\ \alpha_1=\alpha_2=0.01.$

Global Digital Central
ISSN: 2151-8629

5.2 Effect of parameters on temperature profile

Fig. 10 depicts the effect of increasing both the magnetic and the pressure gradient parameters on the temperature profile. As the magnetic field becomes stronger, more work is executed by the fluid to overcome the drag force, so the fluid temperature $\theta(y)$ increases. This accompanying work is then dissipated as thermal energy, heating the fluid and elevating the temperature. Therefore while the transverse magnetic field serves to decelerate fluid flow to achieve flow regulation, a counter-productive effect of heating the fluid is also caused and this requires smart use of magnetic fields so that desired material characteristics are achieved and excessive temperatures are not generated. With decreasing pressure gradient, the temperature of the system decreases, since the fluid friction decreases. Fig. 11 shows the effect of Eckert and suction parameters on the temperature profile.

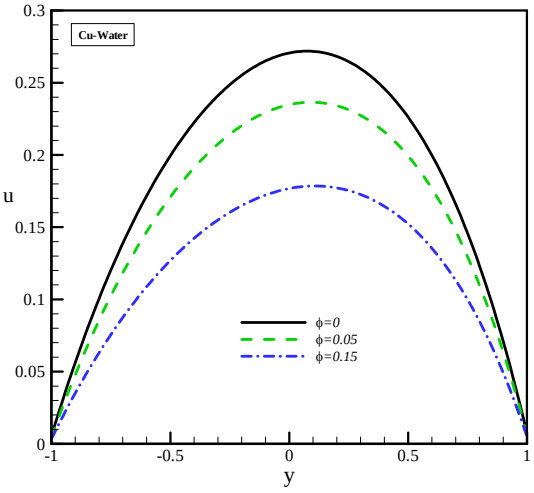

Fig. 8 Effect of ϕ on the velocity profile when $M^2=1,\ P=1,\ S=0.5,\ Ec=0.1,\ \alpha_1=\alpha_2=0.01,\ Bi_1=Bi_2=1.$

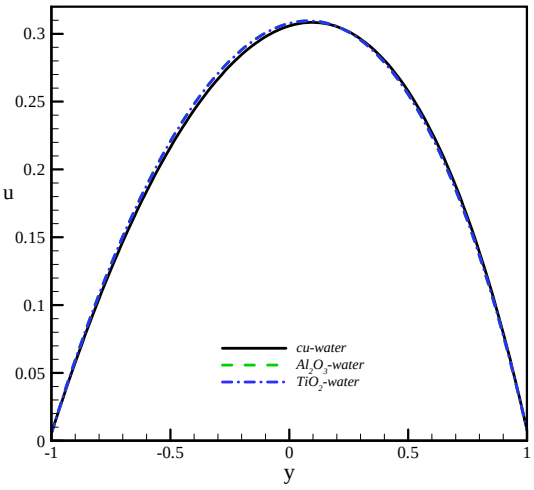

Fig. 9 Effect of water based nanofluids types on the velocity profile when $\phi=0.05,\ M^2=1,\ P=1,\ S=0.5,\ Ec=0.1,\ \alpha_1=\alpha_2=0.01,\ Bi_1=Bi_2=1.$

By increasing Ec, the temperature in the channel increases strongly due to viscous heating. The temperature also increases by increasing the suction parameter, mainly due to an increase in the injection of hot fluid at the lower porous plate.

Fig. 12 depicts the effect of increasing both slip flows on the temperature profile. Generally, the temperature of the system increases with slip flow at the lower plate since fluid friction increases.

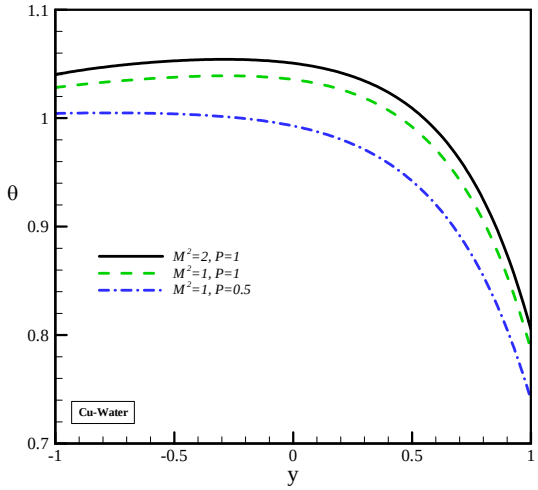

Fig. 10 Effect of M^2, P on the temperature profile when $\phi=0.05,\ S=0.5,\ Ec=0.1,\ \alpha_1=\alpha_2=0.01,\ Bi_1=Bi_2=1.$

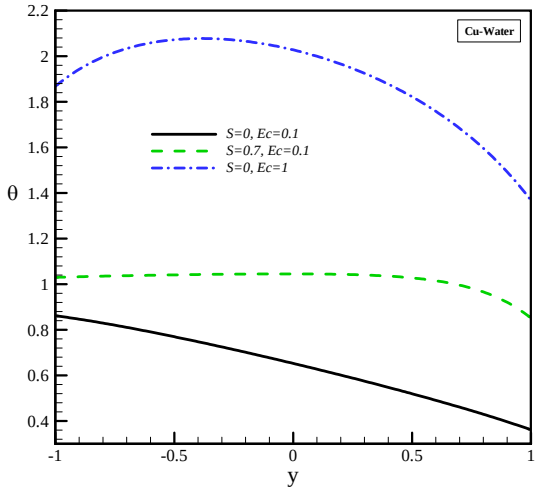

Fig. 11 Effect of S, Ec on the temperature profile when $\phi=0.05,\ M^2=1,\ P=1,\ \alpha_1=\alpha_2=0.01,\ Bi_1=Bi_2=1.$

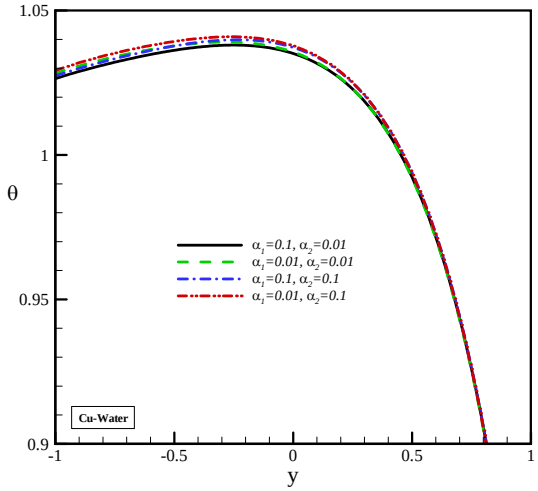

Fig. 12 Effect of α_1, α_2 on the temperature profile when $\phi=0.05,\ M^2=2,\ P=1,\ S=0.5,\ Ec=0.1,\ Bi_1=Bi_2=1.$

Global Digital Central
ISSN: 2151-8629

Fig. 13 demonstrates the effect of the Biot numbers Bi_1 and Bi_2 on fluid temperature. Fluid temperature decreases by increasing Biot number on each side. Biot number is the ratio of the hot fluid side convection resistance to the cold one of a surface. Thus, as Biot numbers increase, the surface temperature increases, since heat transfer to the surroundings is higher.

Fig. 14 shows the effect of the volume fraction of Cu-water, on temperature distribution.

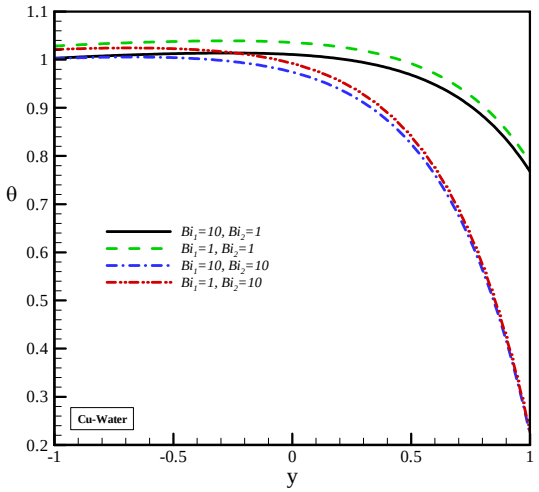

Fig. 13 Effect of Bi_1, Bi_2 on the temperature profile when $\phi = 0.05,\ M^2 = 2,\ P = 1,\ S = 0.5,\ Ec = 0.1,\ \alpha_1 = \alpha_2 = 0.01.$

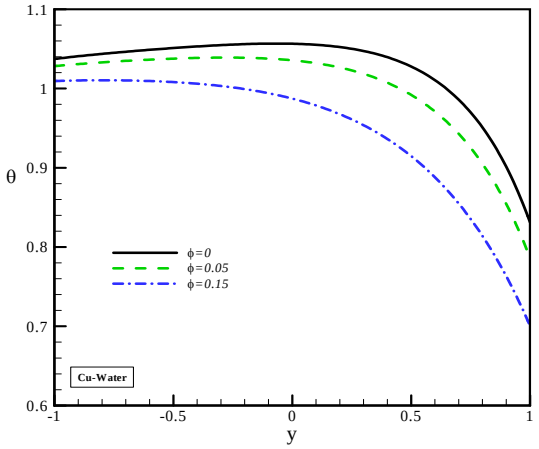

Fig. 14 Effect of ϕ on the temperature profile when $M^2 = 1,\ P = 1,\ S = 0.5,\ Ec = 0.1,\ \alpha_1 = \alpha_2 = 0.01,\ Bi_1 = Bi_2 = 1.$

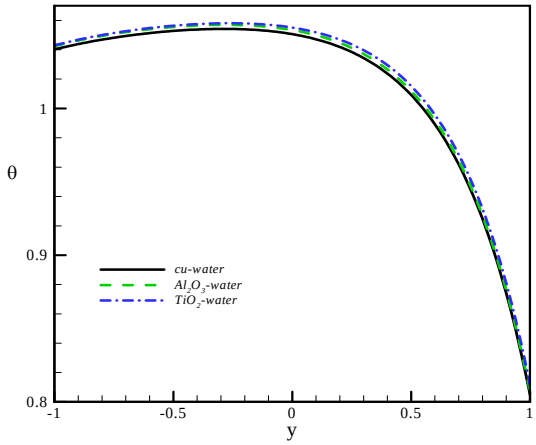

Fig. 15 Effect of water based nanofluids types on the temperature profile when $\phi = 0.05,\ M^2 = 1,\ P = 1,\ S = 0.5,\ Ec = 0.1,\ \alpha_1 = \alpha_2 = 0.01,\ Bi_1 = Bi_2 = 1.$

When the volume fraction of nanoparticles increases, temperature of the fluid decreases which agrees with physical behavior namely when the volume of nanoparticles increases, the thermal conductivity and the rate of heat transfer increases and thus the average temperature will decrease. Fig. 15 presents fluid temperature variations for three types of water based nanofluids, namely Cu-water, Al_2O_3-water and TiO_2-water. The temperature of Cu-water nanofluid is lower than that of Al_2O_3-water and TiO_2-water, because copper has high thermal conductivity, thus the rate of heat transfer increases and the average temperature decreases.

The most important physical quantities, as far as the current research work is concerned are skin friction coefficient and Nusselt number. Their numerical values on the lower and upper plates are shown in the Tables 3 and 4 for several values of nanoparticles volume fraction (ϕ) and suction parameter (S). It is seen from the Table 3 that the skin friction coefficient changes at the plates with an increase in volume fraction of Cu and Al_2O_3 nanoparticles are generally unclear and, of course, negligible. Also, the Nusselt number at the plates decreases with an increase in volume fraction of nanoparticles. Table 4 shows that the skin friction coefficient at the lower plate $(y = -1)$ decreases with an increase in suction parameter whereas it increases at the upper plate $(y = 1)$. The Nusselt number at the lower plate decreases with an increase in suction parameter whereas it increases at the upper plate. It is evident from these two tables that the skin friction coefficient at the lower plate for Al_2O_3 - water nanofluid is greater than Cu - water nanofluid whereas at the upper plate, the result is reversed. In the case of the Nusselt number the results are not much different for Al_2O_3 - water and Cu - water.

Table 3 Effect of volume fraction of nanoparticles on the skin friction coefficient and Nusselt number for Cu and Al_2O_3 nanoparticles.

Volume fraction of nanoparticles (ϕ)	*Cu*				Al_2O_3			
	Skin friction		*Nusselt number*		*Skin friction*		*Nusselt number*	
	Lower plate	*Upper plate*	*Lower plate*	*Upper plate*	*Lower plate*	*Upper plate*	*Lower plate*	*Upper plate*
0	*0.66897*	*1.42459*	*0.04947*	*2.56355*	*0.66897*	*1.42459*	*0.04947*	*2.56355*
0.05	*0.61032*	*1.53679*	*0.03868*	*2.52474*	*0.66720*	*1.42777*	*0.04102*	*2.51594*
0.1	*0.57432*	*1.61366*	*0.02283*	*2.49194*	*0.67116*	*1.42068*	*0.02673*	*2.47422*
0.15	*0.55498*	*1.65766*	*0.00075*	*2.46628*	*0.67996*	*1.40513*	*0.00420*	*2.43940*

Global Digital Central
ISSN: 2151-8629

Table 4 Effect of suction parameter on the skin friction coefficient and Nusselt number for Cu and Al_2O_3 nanoparticles.

suction parameter (S)	*Cu*				Al_2O_3			
	Skin friction		*Nusselt number*		*Skin friction*		*Nusselt number*	
	Lower plate	*Upper plate*	*Lower plate*	*Upper plate*	*Lower plate*	*Upper plate*	*Lower plate*	*Upper plate*
0	*0.99233*	*0.99233*	*0.38920*	*0.64793*	*0.99233*	*0.99233*	*0.38653*	*0.64526*
0.2	*0.82082*	*1.19018*	*0.05335*	*1.36609*	*0.84947*	*1.15300*	*0.05140*	*1.36019*
0.4	*0.67454*	*1.41467*	*0.03251*	*2.15903*	*0.72383*	*1.33170*	*0.03467*	*2.15086*
0.7	*0.49807*	*1.80070*	*0.03346*	*3.17005*	*0.56563*	*1.63311*	*0.03612*	*3.16053*

1. CONCLUSIONS

In this paper the problem of MHD nanofluid flow through a permeable wall channel with hydrodynamic slip and convective boundary conditions in the presence of viscous dissipation and Joule heating has been solved analytically and numerically. To verify the obtained results with those of previously published research, the special case of water as base fluid has also been considered. The results indicate the DTM agrees well with presented numerical results. The following can be concluded:

- In general, by applying a magnetic field, the velocity in the channel decreases and temperature increases.
- Increasing the suction parameter causes the velocity profile to decrease and also to skew toward the upper plate, whereas the temperature increases due to increment in injection of hot fluid at the lower permeable plate.
- Increasing the Eckert number causes the fluid temperature to increase due to viscous heating.
- Increasing the Biot number on each side of the channel causes the fluid temperature to decrease, because heat transfer to the surroundings is higher.

REFERENCES

Abdullah, F.A., 2011, "Theoretical and Experimental Investigation of Natural Composite Materials as Thermal Insulation," *Al-Qadisiya J Eng Sci*, **4**(2), 26-36.

Animasaun, I.L., and Sandeep, N., 2016, "Buoyancy Induced Model for the Flow of 36 nm Alumina-water Nanofluid Along Upper Horizontal Surface of a Paraboloid of Revolution With Variable Thermal Conductivity and Viscosity," *Powder Technology*, **301**, 858-867. http://dx.doi.org/10.1016/j.powtec.2016.07.023

Ayaz, F., 2004, "Solutions of the Systems of Differential Equations by Differential Transform Method," *Applied Mathematics and Computation*, 147, 547-567. http://dx.doi.org/10.1016/S0096-3003(02)00794-4

Babu, M.J., and Sandeep, N., 2016, "3D MHD Slip Flow of a Nanofluid over a Slendering Stretching Sheet with Thermophoresis and Brownian Motion Effects," *J. Molec Liq*, " 222, 1003-1009. https://doi.org/10.1016/j.molliq.2016.08.005

Barletta, A., 1999, "Analysis of Combined Forced and Free Fow in a Vertical Channel with Viscous Dissipation and Isothermal-isoflux Boundary Conditions," *ASME J Heat Transf*, **121**, 349-56. http://dx.doi.org/10.1115/1.2825987

Basiriparsa, A., Rashidi, M.M., Anwar Bég, O., and Sadri, S.M., 2013 "Semi-Computational Simulation of Magneto-hemodynamic Flow in a Semi-porous Channel Using Optimal Homotopy and Differential Transform Methods," *Computers in Biology and Medicine*, **43**, 1142-1153. https://doi.org/10.1016/j.compbiomed.2013.05.019

Chamkha, A.J., 1995, "Hydromagnetic Two-phase Flow in a Channel," *Int. J. Eng. Sci*, **33**, 437-446. No doi available.

Chen, C.K., and Ho, S.H., 1999, "Solving Partial Differential Equations by Two Dimensional Differential Transform Method," *Applied Mathematics and Computation*, **106**, 171-179. https://doi.org/10.1016/S0096-3003(98)10115-7

Chinyoka, T., and Makinde, O.D, 2013, "Analysis of Entropy Generation Rate in an Unsteady Porous Channel Flow with Navier Slip and Convective Cooling," *Entropy*, **15**, 2081-2099.

Choi, S.U.S., and Eastman, J.A., 1995, "Enhancing Thermal Conductivity of Fluids With Nanoparticles," *Materials Science*, **231**, 99-105.

Choi, S.U.S., Zhang, Z.G., Yu, W., Lockwood, F.E., and Grulke, E.A., 2001, "Anomalous Thermal Conductivity Enhancement in Nanotube Suspensions," *Appl. Phys. Lett*, **79**, 2252-2254. https://doi.org/10.1063/1.1408272

Das, S., Banu, A.S., Jana, R.N., and Makinde, O.D., 2015, "Entropy Analysis on MHD Pseudo-plastic Nanofluid Flow through a Vertical Porous Channel with Convective Heating," *Alexandria Engineering Journal*, **54**, 325-337. http://dx.doi.org/10.1016/j.aej.2015.05.003

Das, S.K., Choi, S.U.S., Yu, W., and Pradeep, T., 2007, Nanofluids: Science and Technology, *Wiley, New Jersey*.

Das, S., and Jana, R.N., 2014, "Entropy Generation Due to MHD Flow in a Porous Channel with Navier Slip" *Ain Shams Engineering Journal*, **5**, 575-584. http://dx.doi.org/10.1016/j.asej.2013.11.005

Eegunjobi, A.S., and Makinde, O.D., 2012, "Effects of Navier Slip on Entropy Generation in a Porous Channel with Suction/Injection," *Journal of Thermal Science and Technology*, **7**(4), 522-535. http://dx.doi.org/10.1299/jtst.7.522

Erfani, E., Rashidi, M.M., and Basiriparsa, A., 2010 "The Modified Differential Transform Method For Solving Off-centered Stagnation Flow towards a Rotating Disc," *International Journal of Computational Methods*, **7**(4), 655-670. http://dx.doi.org/10.1142/S0219876210002404

Ibáñez, G., 2015, "Entropy Generation in MHD Porous Channel with Hydrodynamic Slip and Convective Boundary Conditions," *International Journal of Heat and Mass Transfer*, **80**, 274-280. https://doi.org/10.1016/j.ijheatmasstransfer.2014.09.025

Jang, M.J., Chen, C.L., and Liu, Y.C., 2001, "Two-dimensional Differential Transform for Partial Differential Equations," *Applied Mathematics and Computation*, **121**, 261-270.
https://doi.org/10.1016/S0096-3003(99)00293-3

Krishna, P.M., Sandeep, N., Reddy, J.V.R., and Sugunamma, V., 2016, "Dual Solutions for Unsteady Flow of Powell-Eyring Fluid Past an Inclined Stretching Sheet," *Journal of Naval Architecture and Marine Engineering*,**13**(1), 89-99.
http://dx.doi.org/10.3329/jname.v13i1.25338

Li, Q., and Xuan, Y., 2002, "Convective Heat Transfer and Flow Characteristics of Cu-water Nanofluid," *Science in China (Series E)* **45**, 408-416.
http://dx.doi.org/10.1360/02ye9047

Mao, J., Aleksandrova, S., and Molokov, S., 2008, "Joule Heating in Magneto Hydrodynamic Flows in Channels With Thin Conducting Walls," *Int J Heat Mass Transf*, **51**, 4392-4399.
https://doi.org/10.1016/j.ijheatmasstransfer.2008.02.005

Pandey, A.K., and Kumar, M., 2016, "Effect of Viscous Dissipation and Suction/Injection on MHD Nanofluid Flow over a Wedge with Porous Medium and Slip" *Alexandria Engineering Journal* **55**(4), 3115-3123.
http://dx.doi.org/10.1016/j.aej.2016.08.018

Pandey, A.K., and Kumar, M., 2017, "Natural Convection and Thermal Radiation Influence on Nanofluid Flow over a Stretching Cylinder in a Porous Medium with Viscous Dissipation" *Alexandria Engineering Journal* **56**(1), 55-62.
http://dx.doi.org/10.1016/j.aej.2016.08.035

Raju, C.S.K., Sandeep, N., and Malvandi, A., 2016, "Free Convective Heat and Mass Transfer of MHD non-Newtonian Nanofluids over a Cone in the Presence of Non-uniform Heat Source/Sink," *Journal of Molecular Liquids*, **221**, 108-115.
https://doi.org/10.1016/j.molliq.2016.05.078

Rashidi, M.M., BasiriParsa, A., Bég, A.O., Shamekhi, L., Sadri, S.M., and Bég, T.A., 2014, "Parametric Analysis of Entropy Generation in Magneto-Hemodynamic Flow in a Semi-Porous Channel with OHAM and DTM," *Applied Bionics and Biomechanics*, **11**(2), 47-60.
http://dx.doi.org/10.3233/ABB-140086

Rashidi, M.M., Basiriparsa, A., Shamekhi, L., and Momoniat, E., 2015, "Entropy Generation Analysis of the Revised Cheng-Minkowycz Problem for Natural Convective Boundary Layer Flow of Nanofluid in a Porous Medium," *Thermal Science*, **19**, 169-178.
http://dx.doi.org/10.2298/TSCI15S1S69R

Rashidi, M.M., Momoniat, E., Ferdows, M., and Basiriparsa, A., 2014, "Lie Group Solution for Free Convective Flow of a Nanofluid Past a Chemically Reacting Horizontal Plate in a Porous Media," *Math. Prob. Engin*., Volume 2014 (2014), Article ID 239082, 21 pages
http://dx.doi.org/10.1155/2014/239082

Ravikumar, V., Raju, M.C., and Raju, G.S.S., 2012, "MHD Three Dimensional Couette Flow Past a Porous Plate with Heat Transfer," *IOSR J Maths*, 1(3), 3-9.
http://dx.doi.org/10.9790/5728-0130309

Reddy, N. A., Varma, S.V.K., and Raju, M.C., 2009, "Thermo Diffusion and Chemical Effects with Simultaneous Thermal and Mass Diffusion in MHD Mixed Convection Flow with Ohmic Heating,' *J. Naval Architect Mar Eng*, **6**(2), 84-93.
http://dx.doi.org/10.3329/jname.v6i2.3761

Saha, S., Saha, G., Islam, Md. Q., and Raju, M.C., 2010, "Mixed Convection Inside a Lid-driven Parallelogram Cavity with Isoflux Heating," *J Future Eng Technol*, **6**(1), 14-22.
.

Teamah, M.A., 2008, "Numerical Simulation of Double Diffusive Natural Convection in Rectangular Enclosure in the Presences of Magnetic Feld and Heat Source," *Int. J. Therm. Sci*, **47**, 237-248.
https://doi.org/10.1016/j.ijthermalsci.2007.02.003

Upreti, U., Pandey, A.K., and Kumar, M., 2017, "MHD Flow of Ag-water Nanofluid over a Flat Porous Plate with Viscous Ohmic Dissipation, Suction/Injection and Heat Generation/Absorption," *Alexandria Engineering Journal*, **in press.**.

Vyas, P., and Soni, S., 2016, "Entropy Analysis for MHD Casson Fluid Flow in a Channel Subjected to Weakly Temperature Dependent Convection Coefficient and Hydrodynamic Slip," *J. Rajasthan Academy of Physical Sciences*, **15**(1-2), 1-18.

Zhou, J.K., 1986, "Differential Transformation and Its Applications for Electrical Circuits" *Huazhong University Press, Wuhan, China*, (in Chinese)